TEPES
TURKISH JOURNAL OF
ELECTRICAL POWER
AND ENERGY SYSTEMS

TEPES, Vol. 5, Issue. 2, 114-124, 2025 **DOI:** 10.5152/tepes.2025.25001

RESEARCH ARTICLE

In-Situ Efficiency Estimation of Induction Motors Using Whale Optimization Algorithm

Murat Göztaş[1], Mehmet Çunkaş[2], Mehmet Akif Şahman[2]

[1]Department of Electricity and Energy, Kemal Akman Vocational School, Necmettin Erbakan University, Konya, Türkiye
[2]Department of Electrical and Electronics Engineering, Selçuk University Faculty of Technology, Konya,Türkiye

Cite this article as: M. Göztaş, M. Çunkaş, and M.A. Şahman, "In-situ efficiency estimation of induction motors using whale optimization algorithm," *Turk J Electr Power Energy Syst.*, 2025; 5(2), 114-124.

ABSTRACT

This paper investigates the in-situ efficiency prediction of induction motors using four optimization algorithms: genetic algorithm (GA), particle swarm optimization (PSO), whale optimization algorithm (WOA), and red fox optimization algorithm (RFO). Experimental evaluations were conducted on three induction motors with power ratings of 22 kW, 30 kW, and 132 kW under varying load conditions (25%, 50%, 75%, and 100%). The performance of the algorithms is tested not only under full load conditions but also under partial load conditions. This is an important requirement, given that motors usually do not run at full load in real-world applications. The algorithms were assessed based on their convergence behavior, accuracy, and experimentally measured efficiency values. The results revealed that the performance of the algorithms varies depending on the motor power and load level. While WOA is more successful at medium and high loads, PSO stands out at low loads. While GA provides higher accuracy, especially at full load on an motor, the performance of RFO varies according to the load level. In general, the performance of WOA and RFO stands out to some extent. The study demonstrates the advantages of non-intrusive methods for motor efficiency prediction that eliminate the need for direct shaft power measurements. It also offers practical benefits in industrial applications, such as reducing downtime and improving energy management.

Index Terms—Genetic algorithms, induction motor, in situ efficiency estimation, particle swarm optimization, red fox optimization algorithm, whale optimization algorithm

I. INTRODUCTION

As industrialization increases worldwide, energy demand and the environmental impact of power systems have increased the need for sustainable solutions, and energy efficiency has become vital. The industrial sector accounts for the largest share of electricity consumption, and induction motors consume a significant portion of the electricity produced in industrialized and developing countries. These motors play a critical role in the industry and are often used in mechanical handling and processing applications such as pumping, air conditioning, and transmission systems. Optimizing the performance of these motors saves both energy and costs. In addition, on-site evaluation of motor efficiency offers a significant advantage in reducing downtime, identifying motors with low efficiency, and taking appropriate action [1, 2]. Replacing an existing motor with a new, more efficient one can provide significant energy savings; however, the efficiency of existing machines must be determined with high accuracy and low intrusiveness under actual operating conditions [3]. However, precisely determining the energy efficiency of the induction motor requires the measurement of shaft power, which is intrusive and costly [4]. Several less intrusive methods have been proposed for in-situ efficiency estimation of induction machines without measuring shaft power. These methods include the Nameplate method [5], Slip method [6], Current method [7], Equivalent circuit method [8], Segregated loss method [9], Torque method [10], and Optimization-based methods [11].

Recently, optimization-based efficiency determination methods using metaheuristic algorithms have become popular. Pillay, Levin [12] presented a new method for in-situ induction motor efficiency determination using a genetic algorithm (GA). A comparative analysis of the torque meter results was carried out. Sakthivel et al. [13] developed non-intrusive efficiency estimation methods for industrial motors using an immunity algorithm. This method provides a solution to prevent energy wastage. Çunkaş and Sağ [14]

Received: January 7, 2025
Revision Requested: January 13, 2025
Last Revision Received: January 20, 2025
Accepted: February 4, 2025
Publication Date: April 7, 2025

Corresponding author: Mehmet Cunkas mcunkas@selcuk.edu.tr

Content of this journal is licensed under a Creative Commons Attribution (CC BY) 4.0 International License.

determined the efficiency of induction motors using multi-objective evolutionary algorithms. Non-dominated sorting GA-II and Pareto Evolutionary Algorithm-2 were used. Thangaraj et al. [15] employed particle swarm optimization (PSO) and differential evolution techniques to determine the efficiency of induction motors without no-load testing. Comparative analyses were carried out using GAs. Arslan et al. [16] estimated the equivalent circuit parameters of induction motors using a differential evolution algorithm and GA. The results show that the differential evolution algorithm provides higher accuracy. Chandrakanth et al. [17] calculated the in-situ efficiency of induction motors without no-load testing using PSO and validated it with efficiency measurements. Chayakulkheeree et al. [18] devised a methodology based on PSO for three-phase induction motors, demonstrating that efficiency can be estimated without disrupting the operation of the motor through the utilization of fundamental electrical instruments, including clamp-on power meters and non-contact tachometers. Al-Badri et al. [19] presented a method for estimating the efficiency of three-phase induction motors using GA and IEEE Form F2-method F1 calculations. This technique uses a DC test, full load operating point rms voltages, currents, input power, and sensorless speed determination techniques for in-situ efficiency estimation. Bijan and Pillay [20] developed a method based on PSO to reduce the adverse effects of temperature increases on efficiency determination. This method allows efficiency estimation without waiting for thermal stabilization. Diarra et al. [21] developed a hybrid algorithm that reduces the computational load and estimates motor efficiency using Quantum PSO and trust region algorithm (QPSO-TRA). The rotor slot harmonic frequency method estimates the motor speed. Rajesh et al. [22] proposed an efficiency prediction model for induction motors by combining a barnacles mating optimizer and radial basis function neural network. The proposed method is compared with existing techniques, such as GA. This technique enables an accurate performance assessment by optimizing the parameters of the motor.

This paper fills a significant gap by analyzing the performances of these algorithms in detail under different load conditions. As far as we know, there is no literature study that compares optimization techniques such as GA, PSO, the whale optimization algorithm (WOA), and red fox optimization algorithm (RFO) together. Three different motor configurations of 22 kW, 30 kW, and 132 kW are considered, and the algorithms are evaluated based on their convergence behavior, accuracy, and experimentally measured efficiency values. It is observed that the GA and RFO algorithms exhibit slower convergence in some experiments despite their initial low error rates. On the other hand, it is noteworthy that the PSO and WOA algorithms converge faster and predict with high accuracy, even under low load conditions. These findings can be used to fulfill the need to predict the performance of motors accurately. In addition, non-intrusive prediction of motor efficiency offers significant advantages for businesses in reducing downtime and optimizing energy costs. The proposed method provides substantial benefits in industrial applications by providing accurate results without interrupting motor operation. The selection of appropriate algorithms has been shown to have a significant impact on the success of the method and the precise determination of energy efficiency.

Main Points

- Genetic algorithm, particle swarm optimization, whale optimization algorithm, and red fox optimization algorithms were compared for in-situ efficiency estimation of induction motors.
- Experimental evaluations were performed on three induction motors (22 kW, 30 kW, and 132 kW) under 25%, 50%, 75%, and 100% load conditions.
- While WOA and RFO generally performed similarly at low and medium loads, PSO and GA were superior at certain loads
- Particle swarm optimization and WOA algorithms converge quickly, while GA typically exhibits the slowest convergence.
- The non-intrusive estimation method enables accurate efficiency calculations without interrupting motor operation.

II. METHODOLOGY

A. Optimization Algorithms

Optimization algorithms are instrumental in addressing many engineering challenges, whether they originate from practical, real-world applications or the scientific research field [23]. Heuristic optimization algorithms employ mathematical modeling of intelligent behaviors observed in living beings or natural phenomena to solve complex problems. Heuristic optimization algorithms are frequently used in large and complex problems, whereas deterministic methods (such as linear programming) that guarantee global optimality are challenging to solve [24]. Heuristic algorithms are more straightforward to model and apply to complex problems than deterministic optimization approaches. Despite not guaranteeing global optimality, heuristic algorithms can frequently produce operational and high-quality solutions [25]. Therefore, they have attracted the attention of numerous researchers. Heuristic optimization continues to evolve, with new algorithms being proposed and utilized to address various problems. The following is an overview of the optimization algorithms used in experimental studies.

1) Genetic Algorithm:

Holland's GA is recognized as one of the essential cornerstones of heuristic algorithms. It has been employed in numerous complex optimization problems by emulating the evolutionary process observed in biological life and has yielded successful outcomes. The GA is adaptable due to its structure and robust due to the quality of the solutions obtained. Furthermore, it is an approach that can be utilized for continuous and discrete optimization problems [26].

Based on biological evolution principles, GAs utilize a set of operators, including selection, crossover, and mutation, to generate and reproduce the fittest individuals. The process begins with potential solutions randomly generated in the solution space and having a set of genes that can represent the solution.

$$\overrightarrow{X_i} = \vec{L} + rand\left[0,1\right] * \left(\vec{H} - \vec{L}\right) \tag{1}$$

where $\overrightarrow{X_i}$ is the gene vector of individual ith, $\vec{L}$ and $\vec{H}$ are the lower bound and upper bound values, respectively, and rand is a random number in the closed range [0,1].

Every optimization problem has an objective function, and the fitness value is calculated using the objective function of randomly generated individuals. The roulette wheel selection mechanism, which represents one of the selection mechanisms utilized in GA, assigns each individual a specific probability of selection proportional to its fitness value. The selected individuals are then transmitted to the subsequent generation.

$$O_i = \frac{U_i}{\sum_{j=1}^{n} U_j} \tag{2}$$

where O_i represents the probability value of the ith individual and U_i represents the fitness value of the ith individual.

A crossover operation is used to mix individuals' genetic codes. In the two-point crossover approach, gene sequences are separated at two defined points, and the gene sequence in the middle is swapped. The crossover points are denoted here as $k1$ and $k2$. The gene sequence change after the crossover operation is given in (3) and (4).

$$B_1 = \left(x_1, x_2, \ldots, x_{k1}, y_{k1+1} \ldots, y_{k2}, x_{k2+1}, \ldots, x_n\right) \tag{3}$$

$$B_2 = \left(y_1, y_2, \ldots, y_{k1}, x_{k1+1} \ldots, x_{k2}, y_{k2+1}, \ldots, y_n\right) \tag{4}$$

One operator that can be used to alter genetic variation at a specific rate is the mutation operator. When utilizing this operator, minor modifications are performed on a randomly selected number of genes. The selected gene is taken, and its value is reversed in (5).

$$x_i \rightarrow 1 - x_i \tag{5}$$

2) Particle Swarm Optimization Algorithm:
The PSO algorithm is a swarm-based algorithm proposed by Kennedy and Eberhart [27]. The algorithm is often preferred because it is easily adaptable and does not have too many design parameters. The PSO algorithm models the foraging process of flocks of birds and fish together [28]. In this algorithm, particles represent potential solutions. Particles are randomly distributed in the solution space and act according to specific rules. In this process, they find their next position in the solution space by using their best solution (pbest) and the best solution in the swarm (gbest). The goal is to reach the global optimum, achieved by updating the particle's position throughout the process.

In the PSO algorithm, the speed value is a significant factor in the process of transitioning from the current position to the subsequent position. Once the velocity value for each particle has been determined, the new position information is obtained by adding the current position to the velocity value (7).

$$\overrightarrow{V^{n+1}} = \overrightarrow{V^n}.\vec{I} + \vec{c_1}.\overrightarrow{rand}.\left(\overrightarrow{pbest^n} - \overrightarrow{X^n}\right) + \vec{c_2}.\overrightarrow{rand}.\left(\overrightarrow{gbest^n} - \overrightarrow{X^n}\right) \tag{6}$$

$$\overrightarrow{X^{n+1}} = \overrightarrow{X^n} + \overrightarrow{V^{n+1}} \tag{7}$$

where the cognitive and social influence coefficients ($\vec{c_1}$ and $\vec{c_2}$) are vectors, while *rand* represents a random number chosen within the range [0,1]. The vector $\overrightarrow{pbest}$, on the other hand, denotes the position of the best solution thus far. The particle so far $\overrightarrow{gbest}$ represents the vector of the position of the best solution obtained by the swarm at any given point in time. The number of iterations is represented by n, the velocity value of the particle is represented by $\vec{V}$, and the position of the particle is represented by $\vec{X}$. $\vec{I}$ is the inertia coefficient vector.

If the new location produces a better-quality solution than the current location, the particle updates the current location information with the new one. If the solution obtained with the updated position information of any particle is better than the global solution, the global best solution is updated. The last gbest value is the best result obtained when the stop criterion is reached.

3) Whale Optimization Algorithm:
In 2016, Mirjalili and Lewis [29] proposed a WOA, a heuristic algorithm inspired by the hunting strategies of humpback whales. The hunting strategy employed by humpback whales is referred to as the "bubble net attacking" strategy [30]. This strategy involves encircling and compressing their nets, enabling them to hunt their prey through spiral movements. In this approach, the process of locating and searching for prey is regarded as the exploration phase, while the circular maneuvering and compression process is considered the exploitation phase. The success of WOA is based on its ability to execute the exploration and exploitation phases in a balanced manner [31].

In WOA, the prey is initially identified through random searches within the solution space. These searches contribute to the global search, which in turn facilitates a more comprehensive exploration of the solution space. Once they have spotted their prey, humpback whales need to squeeze them. The shrinking encircling mechanism is considered localized foraging. The circular movement of the whale around its prey is realized by the following process. Thus, the whales circle the best solution obtained so far and try to get better solutions by narrowing the prey circle.

$$\vec{F} = \left|\vec{P}.\overrightarrow{B^n} - \overrightarrow{X^n}\right| \tag{8}$$

$$\overrightarrow{X^{n+1}} = \overrightarrow{X^n} - \vec{U}.\vec{F} \tag{9}$$

where $\vec{X}$ is the location vector of the current whale, $\vec{B}$ is the location vector of the whale with the best solution found so far, $\vec{P}$ and $\vec{U}$ are multiplier vectors scaled by random numbers between 0 and 2, n is the number of iterations, and $\vec{F}$ is the distance between the current whale and the whale with the best solution.

$$\overrightarrow{X^{n+1}} = \left|\overrightarrow{B^n} - \overrightarrow{X^n}\right|.e^{sk}.\cos\left(2\grave{A}\mathrm{l}\right) + \overrightarrow{B^n} \tag{10}$$

In the bubble net attacking strategy, whales make a spiral updating position and a shrinking encircling. The choice between these two approaches depends on the random probability p. If p is less than 0.5, the shrinking encircling approach is used; otherwise, the spiral updating position is used. In (10), s is a coefficient acting on the logarithmic spiral, and k is a randomly chosen number in the range [−1,1].

4) Red Fox Optimization Algorithm:
Foxes, which have high adaptation and integration skills, can survive in many geographies around the world [32]. In particular, their high success in hunting approaches allows them to survive even in the most challenging environments [33]. Mohammed and Rashid proposed the RFO algorithm by modeling the prey detection and hunting approaches of red foxes [34]. Red foxes first use sound waves from their potential prey to locate them and then decide in which direction to attack them. If these two processes are well executed, they are highly successful. Sound waves are used by red foxes to detect the distance of prey. The distance between the red fox and potential prey is given by the following equations. The distance between the red fox and the prey is determined by considering the back-and-forth of the detected sound.

$$W = \overrightarrow{bP} / \vec{t}_i \tag{11}$$

$$\vec{M}_i = W * \vec{t}_i \tag{12}$$

$$\overrightarrow{MA}_i = 0.5 * \vec{M}_i \tag{13}$$

where $\vec{t}_i$ is a vector of random numbers in the interval [0,1], W is the speed of sound, $\overrightarrow{bP}$ is the parameter of the best solution found so far. $\vec{M}_i$ symbolizes the reach value of the sound vector that gives the distance to the prey. But $\vec{M}_i$ must be divided by 2 to find the actual distance ($\overrightarrow{MA}_i$). Red foxes use the following equations to determine how to approach and attack prey.

$$J_i = 0.5 * 9.81 * ts^2 \tag{14}$$

$$\vec{X}_{i+1} = \overrightarrow{MA}_i + J_i + a_1 \tag{15}$$

$$\vec{X}_{i+1} = \overrightarrow{MA}_i + J_i + a_2 \tag{16}$$

where ts is the average transfer time of the sound, J_i is the jump position, and 9.81 is the gravity value. The red fox also tries to avoid local optima by obtaining different positions. It updates different positions depending on whether a number in the interval [0,1] is above or below 0.18. If the random value is above 0.18, (5) is used; otherwise, (6) is used.

B. Problem Definition
Fig. 1 shows an induction motor's general equivalent circuit diagram [35]. In this diagram, R_1 and X_1 are stator resistance and reactance, R_2 and X_2 are rotor resistance and reactance, X_m is magnetization reactance, R_{fe} is core loss resistance, s is slip, Pin and $Pout$ are input and output powers, P_{SLL} is leakage losses, and P_{FW} is wind and friction losses. There are seven unknown parameters to estimate the efficiency of the induction motor at any load condition. In addition to these, there are P_{SLL} and P_{FW}. This method reduces the number of unknown parameters to four (X_1, X_m, R_{fe}, and R_2).

1) R_1 Stator Resistance and Temperature:
Stator copper loss accounts for 25–40% of the total losses in the machine, depending on the load. The DC experiment commonly determines it. According to the IEEE Std-112 standard, the following formula can determine R_1 for different load values [36].

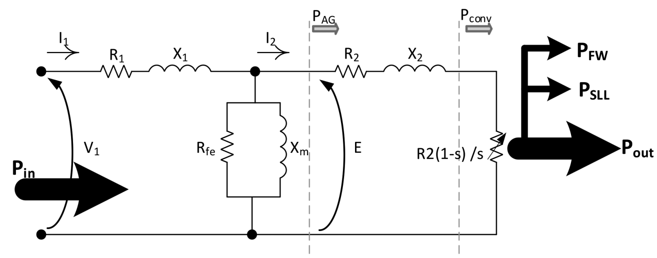

Fig. 1. Induction motor equivalent circuit.

$$R_1 = \frac{R_{1,cold}\left(T_{hot} + K\right)}{T_{cold} + K}, \begin{array}{ll} K = 234{,}5 & \%100\,\text{copper} \\ K = 225 & \text{aluminum} \end{array} \tag{17}$$

where T_{hot} is the operating temperature and T_{cold} is the temperature measured when the motor is cold, or can also be taken as the ambient temperature.

2) X_1 And X_2 Stator and Rotor Reactance:
The reactances X_1 and X_2 are constant and have no relation with temperature variation and load variation. According to the NEMA (National Electrical Manufacturers Association) classification, the X_1 and X_2 parameters of induction motors are distributed as in Table I [19].

3) Rotor Speed and Slip:
Rotor speed can be measured or estimated without contact. Stator current can be determined by harmonic spectrum analysis [37].

4) P_{SLL} Stray Load Losses:
P_{SLL} is load-dependent and represents the eddy current losses in metal components other than conductors. It is very cumbersome to measure directly; the rotor has to be removed, and reverse direction tests have to be performed [38].

5) IEEE standard defining test procedures (IEEE Std-112):

$$P_{SLL} - \Delta P - \left(P_{scl} + P_{fe} + P_{rcl} + P_{FW}\right) \tag{18}$$

6) IEC standard specifying test methods for determining the efficiency and losses of rotating electrical machines (IEC 60034-2):

TABLE I.
DISTRIBUTION OF X_1 AND X_2 PARAMETERS ACCORDING TO NEMA CLASSIFICATION

Motor Class	X_1	X_2
A	0.5	0.5
B	0.4	0.6
C	0.3	0.7
D	0.5	0.5
Rotor winding	0.5	0.5

$$P_{SLL} = P_{in,fl}\left[0.025 - 0.005\log_{10}\left(\frac{P_{out}}{1kW}\right)\right] \tag{19}$$

7) P_{FW} Wind and Friction Losses:

P_{FW} consists of two losses. The first of these is frictional loss, which occurs in the motor shaft and bearings. The second is wind loss, which is due to the motor cooling impeller. It is important to note that both frictional and wind losses vary quadratically with the speed of the induction motor. Furthermore, frictional and wind losses range from 5% to 15% of the total losses, and they can be determined by a no-load running test [36]. In this study, the following approaches were used [19].

$$\begin{aligned} P_{FW} &= 2.5\% \times P_{\text{in,fl}}, \text{2poles} \\ P_{FW} &= 1.2\% \times P_{\text{in,fl}}, \text{4poles} \\ P_{FW} &= 1.0\% \times P_{\text{in.fl}}, \text{6poles} \end{aligned} \tag{20}$$

8) Objective and Fitness Function:

Real and imaginary components of current, input power, and power factor are used as objective functions. f_1 is the ratio of the measured input current and the fundamental components of the estimated input current, f_2 is the ratio of the measured input current and the imaginary components of the estimated input current, f_3 is the ratio of the measured active input power and the estimated active input power, f_4 is the ratio of the measured reactive input power and the estimated reactive input power [19].

TABLE II.
NAMEPLATE DATA OF INDUCTION MOTORS

Power (kW)	22	30	132
V_{LL} (V)	500	500	500
I_L (A)	33.97	49.94	191.33
F (Hz)	50	50	50
Connection type	Δ	Δ	Δ
Rated speed (rpm)	987	992	1493
NEMA design	B	A	A
Number of poles	6	6	4

$$f_1 = \frac{real\left(I_{1,meas}\right) - real\left(I_{1,est}\right)}{real\left(I_{1,meas}\right)} \tag{21}$$

$$f_2 = \frac{imag\left(I_{1,meas}\right) - imag\left(I_{1,est}\right)}{imag\left(I_{1,meas}\right)} \tag{22}$$

$$f_3 = \frac{P_{in,meas} - P_{in,est}}{P_{in,meas}} \tag{23}$$

TABLE III.
LOADED OPERATING EFFICIENCY VALUES OF MOTORS ACCORDING TO TEST REPORTS

22 kW							
Load (%)	**V1 (V)**	**I1 (A)**	**Pi (W)**	**Cos α**	**Speed(rpm)**	**Po (W)**	**Efficiency (%)**
25%	500	17.22	6105	0.41	996	5477	89.7
50%	500	21.51	11 765	0.63	993	10 966	93.2
75%	500	27.13	17 516	0.74	989	16 452	93.9
100%	500	33.57	23 408	0.80	985	21 949	93.8
30 kW							
Load (%)	**V1 (V)**	**I1 (A)**	**Pi (W)**	**Cos α**	**Speed(rpm)**	**Po (W)**	**Efficiency (%)**
25%	500	29.77	8590	0.33	998	7502	87.3
50%	500	34.43	16 240	0.54	995	14 979	92.2
75%	500	41.10	24 008	0.67	993	22 453	93.5
100%	500	49.17	31 919	0.75	991	29 907	93.7
132 kW							
Load (%)	**V1 (V)**	**I1 (A)**	**Pi (W)**	**Cos α**	**Speed(rpm)**	**Po (W)**	**Efficiency (%)**
25%	500	97.43	36 554	0.43	1498	32 942	90.1
50%	500	121.53	69 528	0.66	1496	65 533	94.3
75%	500	153.76	103 013	0.77	1495	98 378	95.5
100%	500	190.83	137 171	0.83	1493	131 565	95.9

TABLE IV.
PARAMETER SETTINGS OF THE ALGORITHMS

GA	PSO	WOA	RFO
Population size = 200 Iteration number = 200 Mutation probability = 0.1 Crossover probability = 0.8	Particle number = 200 Iteration number = 200 C1 = C2 = 2 wmax = 0.9 wmin = 0.4	Population number = 200 Iteration number = 200	Population number = 200 Iteration number = 200 C1 = 0.18 C2 = 1

$$f_4 = \frac{\varphi_{1,meas} - \varphi_{1,est}}{\varphi_{1,meas}} \tag{24}$$

$$\text{Fitness function } : ff_1 = |f_1| + |f_2| + |f_3| + \tag{25}$$

III. RESULTS AND DISCUSSIONS

GA, PSO, WOA and RFO are used to determine the induction motor equivalent parameters, and the performance of these algorithms is compared. Three three-phase 380 V, 50 Hz, 22 kW, 30 kW, and 132 kW induction motors are selected. The nameplate data of these motors are given in Table II. Only the data obtained from the experiments of the motors given in Table III were used for motor parameterization. The experimental data include a comprehensive set of data reflecting the performance of the motor at various load points.

The algorithms need an initial value for the stator resistance R_1. This value is measured directly by direct current testing when the motor

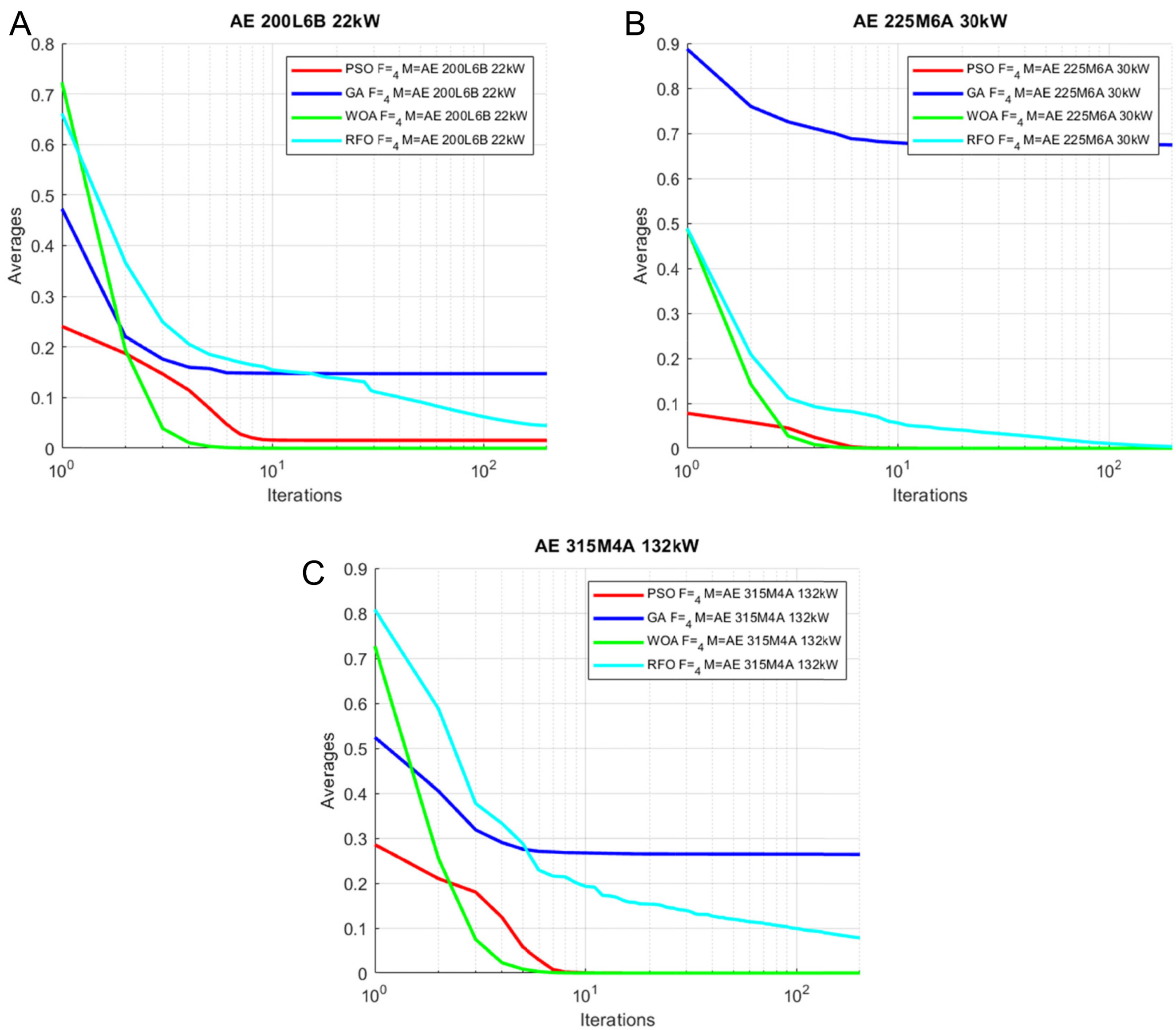

Fig. 2. Convergence of GA, PSO, RFO, and WAO algorithms.

is not running. Then, during the identification process, the effect of temperature rise on the resistance is considered using thermal coefficients, and the R_1 value is updated. Temperature correction is a critical factor affecting motor performance and is especially important to provide more accurate predictions under high current loads. The other four parameters (X_1, X_m, R_{fe}, and R_2) will be determined through optimization algorithms. These parameters are the key components used to build the equivalent circuit model of the motor and are necessary to calculate the performance and efficiency values of the motor accurately.

Equivalent circuit parameters are encoded as real numbers in the algorithm and included in the optimization process in this way. The parameter settings of the algorithms are the factors that directly affect the success of the optimization process, and these settings are given in Table IV. The choice of appropriate parameter settings plays a critical role, especially in finding the global minimum and avoiding the adverse effects of early convergence of the algorithms.

The error difference between the measured data and the values calculated from the estimated parameters was the main criterion for calculating the fitness function. The fitness function in (25) was used to optimize parameters and estimate efficiency. The algorithms were run until a predetermined stopping criterion was reached. This criterion usually depends on factors such as the number of iterations, the error value going below a specific limit value, or improving the solution stopping. Fig. 2 shows in detail the convergence behavior of the algorithms due to the efforts to find the optimum efficiency. In the analysis of the three motors, it was found that the PSO and WOA converged faster than the other algorithms. While the RFO algorithm converges quicker than GA, it still does not match the convergence speed of PSO and WOA. Overall, the GA algorithm tends to converge more slowly compared to the others. The PSO and WOA algorithms are noteworthy for their low error rates and quick convergence features.

Equivalent circuit parameters were generated by four different algorithms: GA, PSO, WOA, and RFO. The calculated values for the real and imaginary components of the motor current, input power, power factor, and output power at each load point were compared with the experimentally measured data. The solution with the smallest error value among the obtained results was selected

TABLE V.
LOADING DATA OF THE MOTORS ACCORDING TO THE DATA OBTAINED FROM THE ALGORITHMS

22 kW									
		PSO		**GA**		**WOA**		**RFO**	
Load (%)	**Actual**	**Estimated**	**Error**	**Estimated**	**Error**	**Estimated**	**Error**	**Estimated**	**Error**
25	89.72	88.88	0.84	91.35	1.63	91.16	1.44	90.92	1.2
50	93.21	92.26	0.95	93.65	0.44	93.48	0.27	93.35	0.14
75	93.92	93.03	0.89	94.09	0.17	93.88	0.04	93.79	0.13
100	93.77	93.09	0.68	94	0.23	93.73	0.04	93.67	0.1
30 kW									
Load (%)	**Actual**	**PSO**		**GA**		**WOA**		**RFO**	
		Estimated	**Error**	**Estimated**	**Error**	**Estimated**	**Error**	**Estimated**	**Error**
25	87.34	87.12	0.22	88.23	0.89	85.68	1.66	84.86	2.48
50	92.23	91.62	0.61	92.29	0.06	90.56	1.67	90.21	2.02
75	93.52	92.94	0.58	93.42	0.1	92.24	1.28	91.91	1.61
100	93.7	93.39	0.31	93.83	0.13	92.83	0.87	92.6	1.1
132 kW									
Load (%)	**Actual**	**PSO**		**GA**		**WOA**		**RFO**	
		Estimated	**Error**	**Estimated**	**Error**	**Estimated**	**Error**	**Estimated**	**Error**
25	90.12	90.59	0.47	92.17	2.05	91.44	1.32	91.24	1.12
50	94.25	94.03	0.22	94.79	0.54	94.48	0.23	94.38	0.13
75	95.5	95.09	0.41	95.68	0.18	95.4	0.1	95.33	0.17
100	95.91	95.54	0.37	96.02	0.11	95.76	0.15	95.72	0.19

as the optimum solution, and the motor efficiency was calculated based on this solution. Then, the corresponding efficiency values at different load points (100%, 75%, 50%, and 25% load) were calculated separately. Table V shows the predicted motor efficiencies and errors corresponding to different load points obtained for all three motors. Fig. 3 shows the efficiency errors of the results obtained from GA, PSO, WOA, and RFO algorithms. For a 22-kW motor, the WOA algorithm provides the highest accuracy, especially at medium and full load values. While PSO performs effectively at low load levels, RFO achieves better results than WOA at low loads but shows average performance at other load levels. The GA has higher error rates and lower accuracy compared to other algorithms. For the 30-kW motor, the GA algorithm exhibited the highest accuracy performance by providing the lowest error rates at medium (50% and 75%) and full (100%) load levels. The PSO algorithm showed the best performance at low load levels (25%) and moderate accuracy at other load levels. The WOA and RFO algorithms had higher error rates, especially at low and medium load levels, and showed lower accuracy performance compared to the other algorithms. For the 132-kW motor, PSO provided the lowest error rate at low loads (25%). The RFO provided the best results at 50% load, while WOA provided the lowest error rate at 75% load. The GA performed best at full load (100%). While WOA and RFO generally performed similarly at low and medium loads, PSO and GA were superior at certain loads. It is evident, therefore, that a load factor of 25% causes the error to rise for all methods. The motor is operating at a light load of 25%. Since the output power is low and the load point is far from the rated load, the losses are greater at this point, which is not advised because it is useless.

Fig. 4 compares estimated efficiency values with measured efficiency values using GA, PSO, WOA, and RFO. Each figure shows the performance of the algorithms for different motor types and power ratings. For the 22-kW motor, the GA and PSO algorithms start with lower efficiency at the beginning (at low load) but approach the measured values as the load increases. The WOA and RFO algorithms converge to the measured values with a low error in general. For the 30-kW motor, the GA and PSO algorithms start with higher efficiency (at low load) and converge to the measured values as the load increases. However, WOA and RFO converge to the measured values with higher error values than the other two algorithms. For the 132-kW motor, the PSO algorithm predicts closer to the measured values at low loads. The RFO and WOA algorithms initially provide larger efficiency estimates but converge to the measured values as the load increases. Although GA had a large error at 25% load, it performed better than PSO at other load levels.

As the load increases, the efficiency estimates of all algorithms converge quite close to the measured values. In general, it is observed that RFO and WOA algorithms converge faster as the load increases, while the GA algorithm provides higher accuracy at a 30-kW motor. The overall agreement between the measured and estimated values shows that the prediction ability of the algorithms used is satisfactory. The performance of the algorithms is tested not only under full load conditions but also under partial load conditions. This is an essential requirement, given that motors usually do not run at full load in real-world applications. The performance evaluation at partial loads demonstrates the algorithms' generalizability and ability to adapt to different operating conditions. The results demonstrate

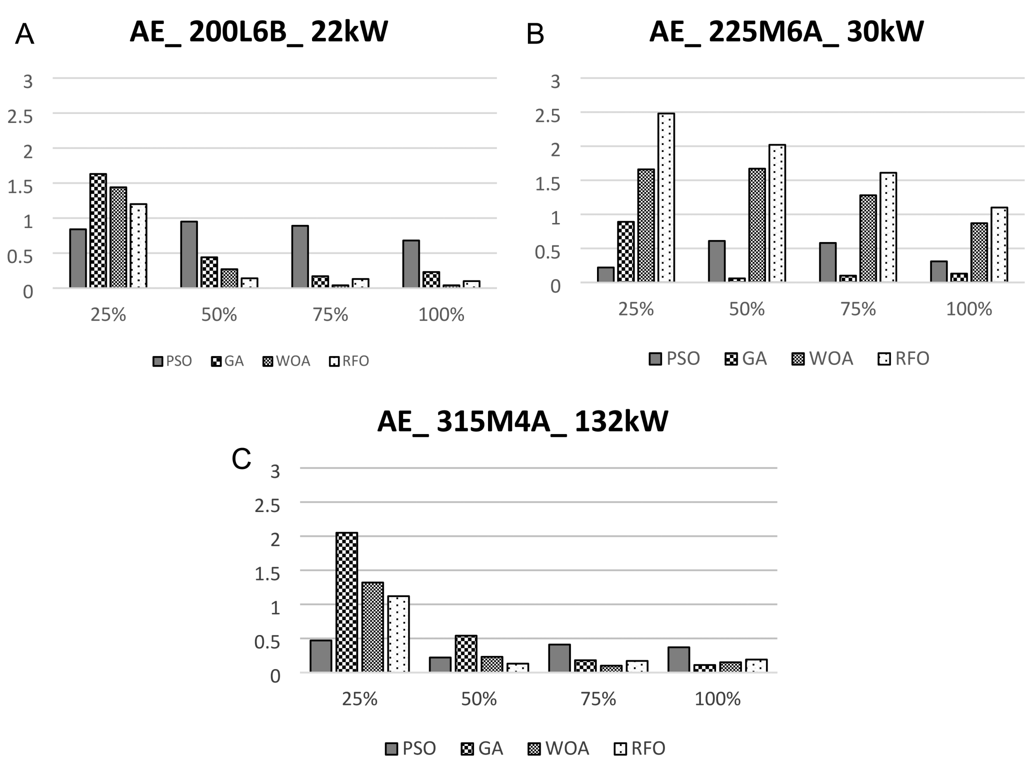

Fig. 3. Efficiency errors of the results obtained from GA, PSO, RFO, and WAO algorithms.

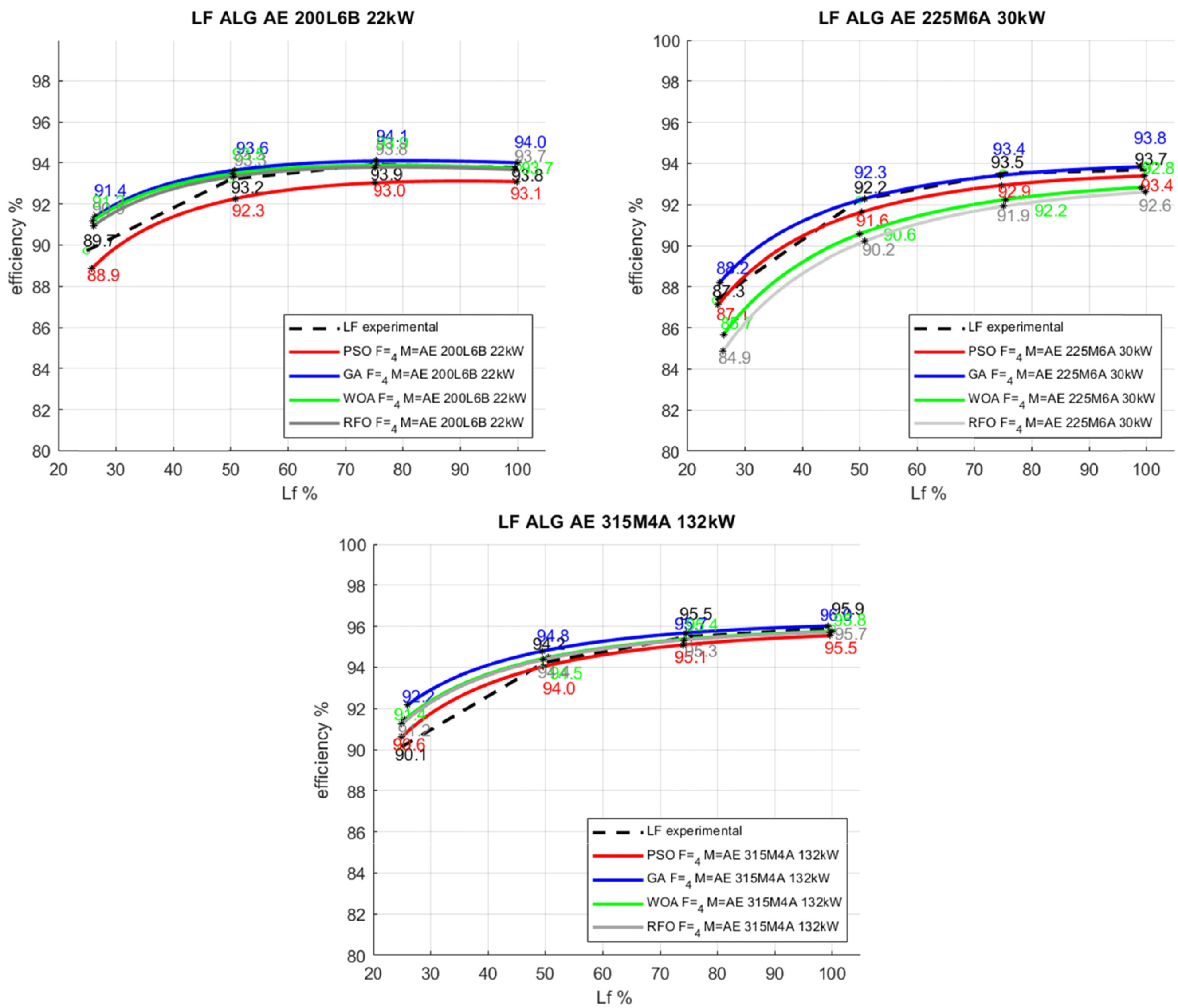

Fig. 4. Efficiency errors of the results obtained from GA, PSO, RFO, and WAO algorithms.

both the accuracy and applicability of the algorithms used to optimize the equivalent circuit parameters of the motor.

IV. CONCLUSIONS

The efficiency estimation of induction motors was analyzed using four optimization algorithms: GA, PSO, WOA, and RFO. Experimental studies were conducted on three induction motors with 22 kW, 30 kW, and 132 kW power ratings at 25%, 50%, 75%, and 100% load points. PSO and WOA algorithms stand out with their fast convergence properties, while RFO showed a slightly slower but still better convergence performance than GA. Although the GA algorithm provided slower convergence in general, it offered high accuracy, especially for the full load conditions of the 30-kW motor and 132-kW motor. For the 22-kW motor, WOA gave the best results at full and medium loads, while PSO showed superior performance at low loads. For the 132-kW motor, PSO provided the lowest error rate at low loads, RFO at medium, and WOA at 75% loads. As the load increased, the prediction accuracies of all algorithms became more consistent with the experimental data, and it was observed that the error rates increased at low loads (especially at 25% load). In general, the algorithms were found to be successful in optimizing the motor equivalent circuit parameters in terms of both accuracy and applicability.

The results highlight the importance of choosing the right algorithms based on motor power and operating load conditions. Furthermore, they demonstrate that non-intrusive efficiency estimation methods offer significant advantages in industrial applications. These methods provide accurate results, reduce downtime, identify low-efficiency motors, and enhance energy management.

Availability of Data and Materials: The data that support the findings of this study are available on request from the corresponding author.

Peer-review: Externally peer-reviewed.

Author Contributions: Concept – M.Ç., M.G.; Design – M.Ç., M.G.; Supervision – M.Ç. Resources – M.Ç., M.G., M.A.Ş.; Materials – M.G.; Data Collection and/or Processing – M.G., M.A.Ş.; Analysis and/or Interpretation – M.Ç., M.G., M.A.Ş.; Literature Search – M.G., M.Ç.; Writing – M.Ç., M.G., M.A.Ş.; Critical Review – M.Ç., M.G.

Declaration of Interests: The authors have no conflicts of interest to declare.

Funding: This study received no funding.

REFERENCES

1. G. K. Esen, and E. Özdemir, "A new field test method for determining energy efficiency of induction motor," *IEEE Trans. Instrum. Meas.*, vol. 66, no. 12, pp. 3170–3179, 2017. [CrossRef]
2. J. Rengifo, E. Albanez, J. Benzaquen, A. Bueno, and J. M. Aller, "Full-load range in-situ efficiency estimation method for induction motors using only a direct start-up," in International Conference on Electrical Machines (ICEM). New York, United States of America: IEEE, 2018. [CrossRef]
3. A. G. Siraki, and P. Pillay, "Comparison of two methods for full-load in situ induction motor efficiency estimation from field testing in the presence of over/undervoltages and unbalanced supplies," *IEEE Trans. Ind. Appl.*, vol. 48, no. 6, pp. 1911–1921, 2012. [CrossRef]
4. V. S. Santos, J. J. Cabello Eras, A. Sagastume Gutierrez, and M. J. Cabello Ulloa, "Assessment of the energy efficiency estimation methods on induction motors considering real-time monitoring," *Measurement*, vol. 136, pp. 237–247, 2019. [CrossRef]
5. G. F. V. Amaral, J. M. R. Baccarini, F. C. R. Coelho, and L. M. Rabelo, "A high precision method for induction machine parameters estimation from manufacturer data," *IEEE Trans. Energy Convers.*, vol. 36, no. 2, pp. 1226–1233, 2021. [CrossRef]
6. J. R. Holmquist, J. A. Rooks, and M. E. Richter, "Practical approach for determining motor efficiency in the field using calculated and measured values," *IEEE Trans. Ind. Appl.*, vol. 40, no. 1, pp. 242–248, 2004. [CrossRef]
7. S. John, D. John, and O. MITCHELL, "Comparison of induction motor field efficiency evaluation method," *IEEE Trans. Ind. Appl.*, vol. 34, no. 1, 1998.
8. B. Lu, T. G. Habetler, and R. G. Harley, "A survey of efficiency-estimation methods for in-service induction motors," *IEEE Trans. Ind. Appl.*, vol. 42, no. 4, pp. 924–933, 2006. [CrossRef]
9. J. Kueck et al., *Assessment of Methods for Estimating Motor Efficiency and Load under Field Conditions*. OAK RIDGE NATIONAL LABORATORY, 1996.
10. B. Lu, T. G. Habetler, and R. G. Harley, "A nonintrusive and in-service motor-efficiency estimation method using air-gap torque with considerations of condition monitoring," *IEEE Trans. Ind. Appl.*, vol. 44, no. 6, pp. 1666–1674, 2008. [CrossRef]
11. G. S. Grewal, and B. Singh, "Efficiency determination of in-service induction machines using gravitational search optimization," *Measurement*, vol. 118, pp. 156–163, 2018. [CrossRef]
12. P. Pillay, V. Levin, P. Otaduy, and J. Kueck, "In-situ induction motor efficiency determination using the genetic algorithm," *IEEE Trans. Energy Convers.*, vol. 13, no. 4, pp. 326–333, 1998. [CrossRef]
13. V. P. Sakthivel, R. Bhuvaneswari, and S. Subramanian, "Immune algorithm based non-intrusive efficiency determination for in-situ induction motor," *Aust. J. Electr. Electron. Eng.*, vol. 7, no. 1, pp. 31–41, 2010. [CrossRef]
14. M. Çunkaş, and T. Sağ, "Efficiency determination of induction motors using multi-objective evolutionary algorithms," *Adv. Eng. Softw.*, vol. 41, no. 2, pp. 255–261, 2010. [CrossRef]
15. R. Thangaraj, M. Pant, C. T. Raj, and A. K. Nagar, "In situ efficiency determination of induction motor: A comparative study of evolutionary techniques," *Appl. Artif. Intell.*, vol. 25, no. 2, pp. 116–140, 2011. [CrossRef]
16. M. Arslan, M. Çunkaş, and T. Sağ, "Determination of induction motor parameters with differential evolution algorithm," *Neural Comput. Appl.*, vol. 21, no. 8, pp. 1995–2004, 2012. [CrossRef]
17. S. A. Chandrakanth et al., "In-situ efficiency determination of induction motor through parameter estimation," in *Proceedings of the International Conference on Soft Computing for Problem Solving (SocProS 2011)*, vol. 1. Berlin: Springer, 2011, p. 2012.
18. K. Chayakulkheeree, V. Hengsritawat, and P. Nantivatana, "Particle swarm optimization based equivalent circuit estimation for on-service three-phase induction motor efficiency assessment," *Eng. J.*, vol. 21, no. 6, pp. 101–110, 2017. [CrossRef]
19. M. Al-Badri, P. Pillay, and P. Angers, "A novel in situ efficiency estimation algorithm for three-phase IM using GA, IEEE method F1 calculations, and pretested motor data," *IEEE Trans. Energy Convers.*, vol. 30, no. 3, pp. 1092–1102, 2015. [CrossRef]
20. M. G. Bijan, and P. Pillay, "Efficiency estimation of the induction machine by particle swarm optimization using rapid test data with range constraints," *IEEE Trans. Ind. Electron.*, vol. 66, no. 8, pp. 5883–5894, 2019. [CrossRef]
21. M. N. Diarra, Y. Yao, Z. Li, M. Niasse, Y. Li, and H. Zhao, "In-situ efficiency estimation of induction motors based on Quantum Particle Swarm Optimization-Trust Region Algorithm (QPSO-TRA)," *Energies*, vol. 15, no. 13, p. 4905, 2022. [CrossRef]
22. P. Rajesh, F. H. Shajin, and N. V. Anand, "An efficient estimation model for induction motor using BMO-RBFNN technique," *Process Integr. Optim. Sustain.*, vol. 5, no. 4, pp. 777–792, 2021. [CrossRef]
23. R. K. Hamad, and T. A. Rashid, "GOOSE algorithm: A powerful optimization tool for real-world engineering challenges and beyond," *Evolving Syst.*, vol. 15, no. 4, pp. 1249–1274, 2024. [CrossRef]
24. M. Ghasemi, M. Zare, P. Trojovský, R. V. Rao, E. Trojovská, and V. Kandasamy, "Optimization based on the smart behavior of plants with its engineering applications: Ivy algorithm," *Knowl. Based Syst.*, vol. 295, p. 111850, 2024. [CrossRef]
25. Z. Benmamoun, K. Khlie, G. Bektemyssova, M. Dehghani, and Y. Gherabi, "Bobcat Optimization Algorithm: An effective bio-inspired metaheuristic algorithm for solving supply chain optimization problems," *Sci. Rep.*, vol. 14, no. 1, p. 20099, 2024. [CrossRef]
26. J. McCall, "Genetic algorithms for modelling and optimisation," *J. Comp. Appl. Math.*, vol. 184, no. 1, pp. 205–222, 2005. [CrossRef]
27. J. Kennedy, and R. Eberhart, "Particle swarm optimization," in *Proceedings of ICNN'95-International conference on neural networks*. New York, United States of America: ieee, 1995, pp. 1942–1948. [CrossRef]
28. W. Tang, L. Cao, Y. Chen, B. Chen, and Y. Yue, "Solving engineering optimization problems based on multi-strategy particle swarm optimization hybrid dandelion optimization algorithm," *Biomimetics (Basel)*, vol. 9, no. 5, p. 298, 2024. [CrossRef]
29. S. Mirjalili, and A. Lewis, "The whale optimization algorithm," *Adv. Eng. Softw.*, vol. 95, pp. 51–67, 2016. [CrossRef]
30. L. Deng, and S. Liu, "Deficiencies of the whale optimization algorithm and its validation method," *Expert Syst. Appl.*, vol. 237, p. 121544, 2024. [CrossRef]
31. A. M. Ahmed et al., "Balancing exploration and exploitation phases in whale optimization algorithm: An insightful and empirical analysis," in *Handbook of Whale Optimization Algorithm*. Amsterdam: Elsevier, 2024, pp. 149–156. [CrossRef]
32. X.-S. Yang, and X. He, "Nature-inspired optimization algorithms in engineering: Overview and applications," in *Nature-Inspired Computation in*

Engineering, X.-S. Yang, Ed. Cham: Springer International Publishing, 2016, pp. 1–20. [CrossRef]

33. C. D. Soulsbury, P. J. Baker, G. Iossa, and S. Harris, "Fitness costs of dispersal in red foxes (Vulpes vulpes)," *Behav. Ecol. Sociobiol.*, vol. 62, no. 8, pp. 1289–1298, 2008. [CrossRef]
34. H. Mohammed, and T. Rashid, "FOX: A FOX-inspired optimization algorithm," *Appl. Intell.*, vol. 53, no. 1, pp. 1030–1050, 2023. [CrossRef]
35. A. G. Siraki, P. Pillay, and P. Angers, "Full load efficiency estimation of refurbished induction machines from no-load testing," *IEEE Trans. Energy Convers.*, vol. 28, no. 2, pp. 317–326, 2013. [CrossRef]
36. S. C. E. R. L. Mantilla, "How the efficiency of induction motor is measured?," *Energy*, vol. 15, p. 15, 2008.
37. K. D. Hurst, and T. G. Habetler, "A comparison of spectrum estimation techniques for sensorless speed detection in induction machines," *IEEE Trans. Ind. Appl.*, vol. 33, no. 4, pp. 898–905, 1997. [CrossRef]
38. Society, P. E., *IEEE Standard Test Procedure for Polyphase Induction Motors and Generators*. New York, NY: IEEE, 2004.